MR imaging in neurocysticercosis: a study of 56 cases.

H R Martinez, R Rangel-Guerra, G Elizondo, J Gonzalez, L E Todd, J Ancer and S S Prakash

AJNR Am J Neuroradiol 1989, 10 (5) 1011-1019
http://www.ajnr.org/content/10/5/1011

MR Imaging in Neurocysticercosis: A Study of 56 Cases

Hector R. Martinez[1]
Ricardo Rangel-Guerra[1]
Guillermo Elizondo[2]
Jorge Gonzalez[2]
Luis E. Todd[2]
Jesus Ancer[3]
Sharma Shanti Prakash[1]

We reviewed the MR findings in 56 patients with neurocysticercosis (NCC). MR findings were correlated with other neuroradiologic findings in 40 cases, with histopathologic studies in 15 surgically treated patients, and with autopsy findings in one case. Active NCC was characterized by the presence of a cyst in the brain parenchyma (53%) or in an intraventricular subependymal (22%) or subarachnoid (10%) location. The cysticercus appeared as a vesicle with a high-intensity signal nodule that corresponded to the scolex. Cyst mobility was observed in two intraventricular cases. Periventricular edema and ependymitis appeared as high-intensity signal on T2 sequences. Inactive NCC (15%) was characterized by calcifications (signal void on T1 and T2 sequences), aqueductal stenosis, and tissue thickness in the basal meninges. Degenerative cysticercus appeared on MR as an irregular vesicle without a scolex. Active NCC was better detected with MR than with CT (85% vs 21%), whereas inactive forms were observed better with CT (23% vs 14%).

We conclude that MR is sensitive in the diagnosis of active NCC and may be useful in evaluating the degenerative changes in the parasite that occur as a result of natural degeneration, host response, or medical therapy.

AJNR **10:1011–1019, September/October 1989**

Neurocysticercosis (NCC) produces a number of neurologic syndromes induced by CNS infestation of cysticerci, the larvae of *Taenia solium* [1, 2]. It is considered an endemic disease in underdeveloped countries [3, 4]. However, owing to the massive immigration to industrialized countries, the prevalence of this neuroparasitosis has increased markedly in the developed world [5–7]. In some endemic areas, the prevalence of NCC is about 3% of the general population, and it is now considered a public health problem.

The accuracy of the diagnosis of NCC was improved with CT. CT was considered the method of choice in its diagnosis, along with immunologic studies of the CSF, especially the measurement of antibodies against cysticercus antigens through the enzyme-linked immunosorbent assay (ELISA) method [8–11]. However, we have found that the accuracy and reliability in the diagnosis of NCC is improved with the use of MR particularly in the intraventricular, brainstem, intraocular, subarachnoid, spinal, and cerebellar forms of NCC.

Recent reports describe the accuracy of MR in the diagnosis of this neuroparasitosis [11–14]. This article describes the MR findings in 56 cases of NCC. We compared the MR findings with other neuroradiologic studies in 40 cases, with neurosurgical findings in 15 cases, and with CSF analysis and histopathologic data when available.

Materials and Methods

Of the first 2000 MR studies performed at the MR unit of the Hospital Universitario in Monterrey, Mexico, from September 1986 to March 1988, we found 56 patients with the

Received May 27, 1988; revision requested August 2, 1988; final revision received February 20, 1989; accepted February 28, 1989.

[1] Neurology Service, Hospital Universitario, Universidad Autonoma de Nuevo Leon, Apdo. Postal 4469, Monterrey, N. L. Mexico. Address reprint requests to H. R. Martinez.

[2] MRI Unit, Hospital Universitario, Universidad Autonoma de Nuevo Leon, Monterrey, N. L. Mexico.

[3] Department of Pathology, Hospital Universitario, Universidad Autonoma de Nuevo Leon, Monterrey, N. L. Mexico.

0195-6108/89/1005-1011

diagnosis of NCC. Forty-eight patients were managed in the neurology service of our hospital and clinically examined by two of the authors. In the other eight cases, adequate information was obtained from the patients' physicians concerning other neuroimaging studies and medical or surgical treatment.

All MR examinations were performed on a 0.3-T Fonar Beta-3000 MR system, with permanent magnet and head coil. Each patient was examined with axial, coronal, and sagittal T1-weighted, 500/28 (TR/TE), spin-density-weighted, 200/28, and T2-weighted, 2000/84, pulse sequences. The slice thickness was 7 mm with 3-mm interslice gaps. Images were acquired on a 128 × 128 matrix with a 1.7-mm pixel size and were extrapolated to a 256 × 256 matrix for display.

The MR examinations were compared with CT findings in 32 cases, positive-contrast CT cisternography in one case, myelography in one case, and ventriculography in six cases. The CT images were obtained with 8-mm-thick axial slices with and without infusion of contrast material.

The CSF was analyzed in 20 cases: 10 samples were obtained from lumbar punctures and 10 samples from the ventricular system were obtained during the surgical procedure, performed either for removal of an intraventricular cyst or for placement of a ventricular shunt catheter. All CSF samples were sent for glucose, protein, and leukocyte determinations. In 10, the immunoglobulin M antibodies against cysticercus antigens were measured by the ELISA method. In all other cases, the hospital chart or the patients' physicians did not provide information regarding the methodology of testing the antibodies against cysticercus.

Fifteen patients had surgical extirpation of the cyst from different locations, either in supratentorial or infratentorial regions. An ependymal or periependymal tissue biopsy was obtained in three cases, a small arachnoidal sample was obtained in one case, and an autopsy was performed in one case. Most of the histologic work was performed in paraffin-embedded tissues using H and E stains in 7-μm slices.

Medical treatment with albendazole (ABZ) or praziquantel (PZQ) was given in 22 cases according to methodology previously described [7, 10, 15]. After medical or surgical treatment, all patients had repeat MR examinations. In four cases, MR was performed during or soon after medical therapy.

Results

We found 56 cases of NCC in the first 2000 MR examinations, accounting for 2.8% of the total studies. The group comprised 31 males and 25 females 6–65 years old (mean, 31.4 years). The most common symptoms observed in our cases were headache (44.6%), epilepsy (40%), and vomiting (25%). The most frequent clinical signs were related to pyramidal tract dysfunction (28.6%) and papilledema (21.4%).

Most of the patients in this series had an active form of NCC (85%), which was defined by the presence of the cyst. The intracranial cysticerci localized most often in the brain parenchyma (53%). The MR configuration of the cyst consisted of a spherical structure with signal properties closely paralleling those of CSF. Inside the sphere a high-intensity signal nodule corresponding to the scolex was visualized either on T1- (500/28) or T2- (2000/84) weighted images (Fig. 1). In cases of intense host reaction around the cyst, the scolex was not clearly detected on T2 sequences. A high-intensity signal was observed in the periphery of the cyst in most of the parenchymatous NCC cases, indicating the presence of edema.

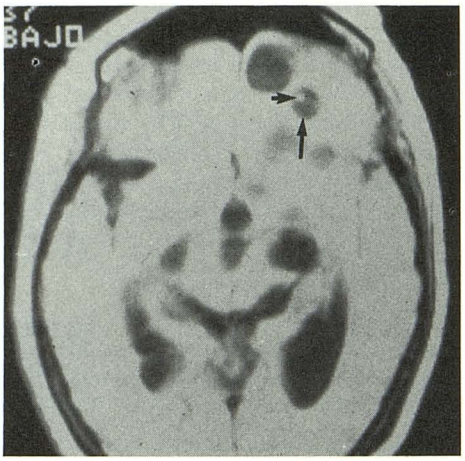

Fig. 1.—Brain parenchymal cysts (500/28 sequence). Vesicle (*large arrow*) is seen as spherical structure with high-signal-intensity nodule (*small arrow*).

Intraventricular NCC was detected in 11 cases (20%), six in the fourth ventricle (Fig. 2A) and five in the lateral ventricle. In two cases of intraventricular NCC, cyst migration in the lateral ventricle was observed when the patient changed position prior to scanning (Figs. 2B–2F). In most of the ventricular NCC cases, a high-intensity signal was detected on T2 sequences in the ependymal layer and subependymal tissue. Histopathologic studies of material obtained at surgery (three cases) and autopsy (one case) demonstrated the presence of ependymitis with periventricular edema and mononuclear inflammatory infiltration.

CT was unable to detect intraventricular NCC either in supratentorial (Fig. 2G) or infratentorial (Fig. 2H) locations. When CT was performed after ventricular injection of contrast material, the ventricular cyst was detected in all but one case (Fig. 3).

Subarachnoid NCC was observed in 10% of the total cases; in two of these, a racemose form of the cyst was present (Fig. 4A). Its configuration was of a multilobular structure, hypointense relative to normal brain on T1-weighted images, several centimeters in size, and lacking a scolex or scoleces. In one case in this series a racemose cysticercus produced an image compatible with a tumoral mass, but surgery corroborated the presence of subarachnoid NCC.

A subependymal cyst was detected in one case and intraspinal NCC was seen in one case at the lumbar level involving the subarachnoid space. Intraocular cysticercus was detected in two patients, both associated with parenchymal NCC (Fig. 5). CT was not performed in these cases. PZQ therapy was given to one patient at another hospital, which resulted in loss of the involved eye. Both cases were corroborated through ophthalmologic examination or surgery.

In active NCC, the cysts were detected more frequently by MR than by CT (85% vs 21%). This was due to better detection of cysts in the subcortical and subarachnoid posterior fossa (Fig. 6). The differentiation between brain edema around the cysts and the previously described cysticercosis

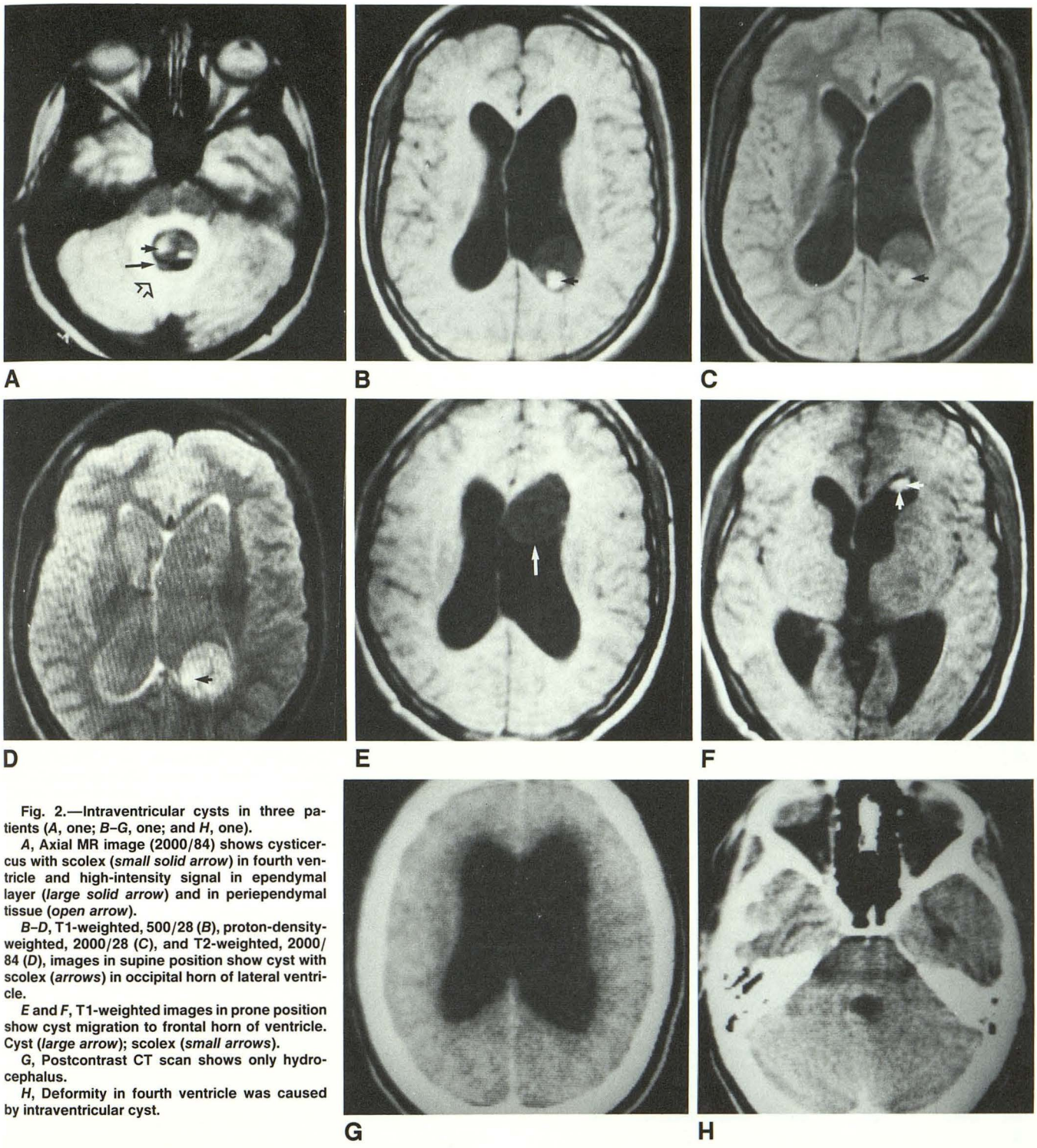

Fig. 2.—Intraventricular cysts in three patients (*A*, one; *B–G*, one; and *H*, one).

***A*, Axial MR image (2000/84) shows cysticercus with scolex (*small solid arrow*) in fourth ventricle and high-intensity signal in ependymal layer (*large solid arrow*) and in periependymal tissue (*open arrow*).**

***B–D*, T1-weighted, 500/28 (*B*), proton-density-weighted, 2000/28 (*C*), and T2-weighted, 2000/84 (*D*), images in supine position show cyst with scolex (*arrows*) in occipital horn of lateral ventricle.**

***E* and *F*, T1-weighted images in prone position show cyst migration to frontal horn of ventricle. Cyst (*large arrow*); scolex (*small arrows*).**

***G*, Postcontrast CT scan shows only hydrocephalus.**

***H*, Deformity in fourth ventricle was caused by intraventricular cyst.**

vasculitis [16] was better observed on postcontrast CT (Fig. 7A). On MR, a high-intensity signal was observed in the periphery of the cyst on T2-weighted images; however, it was not possible to differentiate between perilesional edema and vasculitis (Fig. 7B).

Inactive NCC was present in eight cases (14%). Calcifications were observed as a signal void on T1 and T2 sequences (Fig. 5B). Brain parenchymal calcifications were detected in three cases and were in a subarachnoid location in one (multiple lesions in two). Three patients had aqueductal stenosis, which was seen on MR as a lack of flow void in the aqueduct on sagittal T1- and T2-weighted images. An isointense signal relative to that of the normal brain was observed in the ependymal layer of the aqueduct in these cases. This

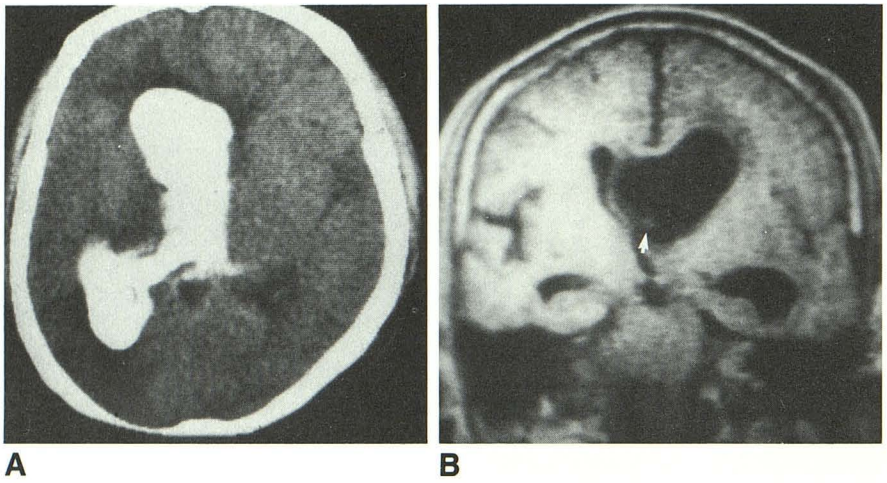

Fig. 3.—Intraventricular cysts.
***A*, CT ventriculogram shows asymmetric hydrocephalus with occlusion of left foramen of Monro.**
***B*, Coronal MR image (500/28) shows cyst in left lateral ventricle with occlusion of left foramen of Monro. Scolex (*arrow*).**

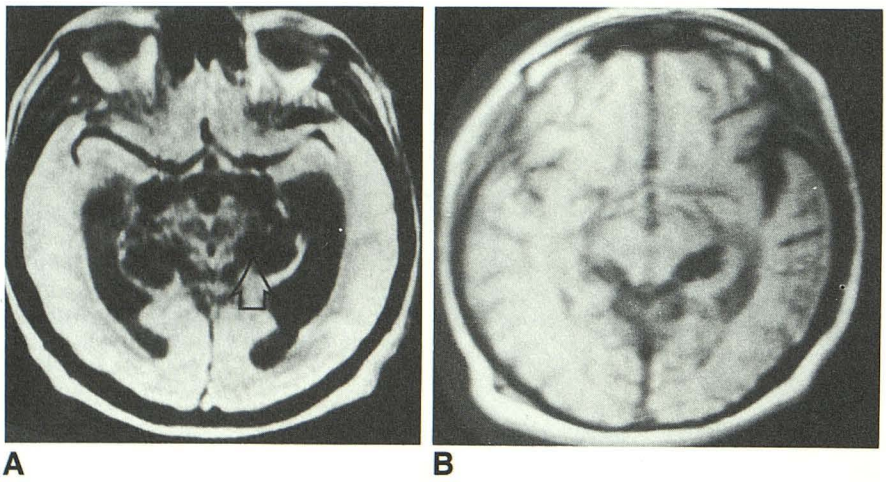

Fig. 4.—Subarachnoid cysts (500/28 images).
***A*, Racemose cyst is hypointense signal of irregular structures filling suprachiasmatic and perimesencephalic cisterns (*arrow*).**
***B*, 3 weeks after ventricular shunting and albendazole therapy.**

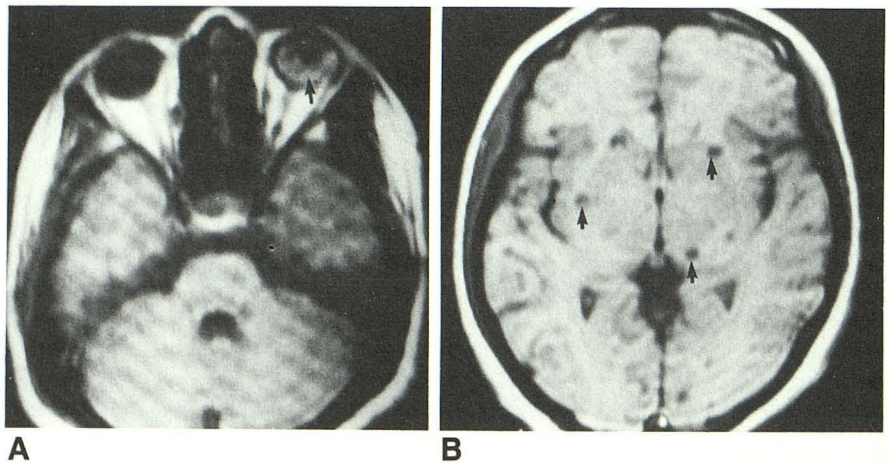

Fig. 5.—Intraocular cyst.
***A*, Left eyeball has cysticercus (*arrow*).**
***B*, Multiple calcifications appear as signal void (*arrows*).**

finding was considered to correspond to chronic ependymitis or ependymal fibrosis, but was not histologically proved. Two patients with hydrocephalus had an isointense signal in the basal meninges associated with tissue thickness on T1 sequences (Fig. 8). We suspect that this finding corresponds to chronic basal arachnoiditis, although histologic proof was lacking.

Degenerative cysts were observed as irregular spheres with less peripheral edema and no scolex (Figs. 9A, 9D, and 9E). In one case, a high-intensity signal was detected within the cyst (Fig. 9A); however, the histologic studies showed only necrotic material (Fig. 9B). Three patients who had the MR findings described above had surgery because of uncontrolled seizures, and the histopathologic examination dem-

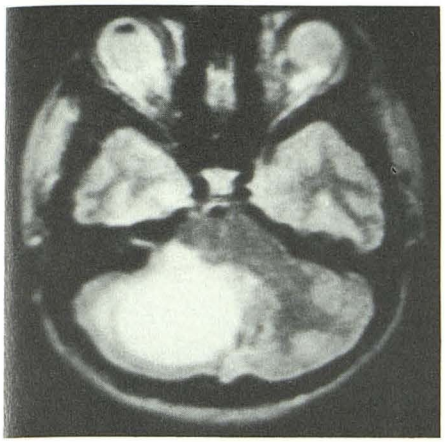

Fig. 6.—Parenchymal cyst.
Axial MR image (2000/84) shows vesicle in right cerebellar hemisphere (racemose cyst). Mild edema or inflammatory reaction is seen around cyst.

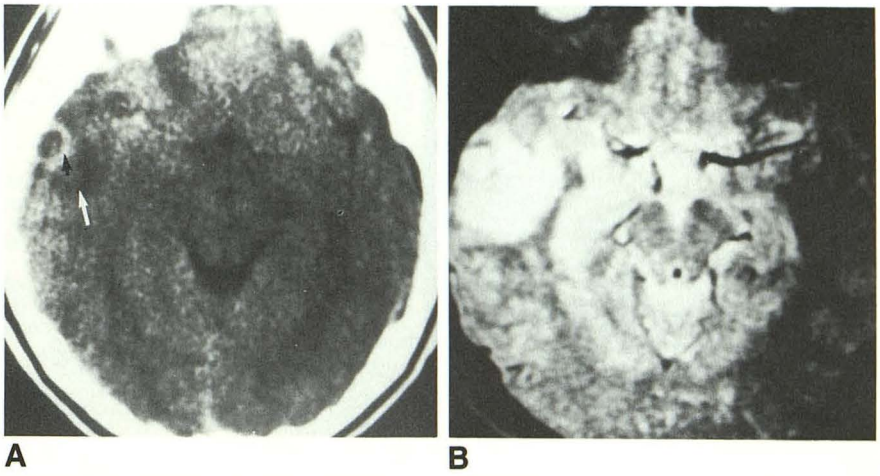

Fig. 7.—Cysticercosis vasculitis (*black arrow*) is better differentiated from brain edema (*white arrow*) on CT scan (*A*) than on corresponding MR image (*B*).

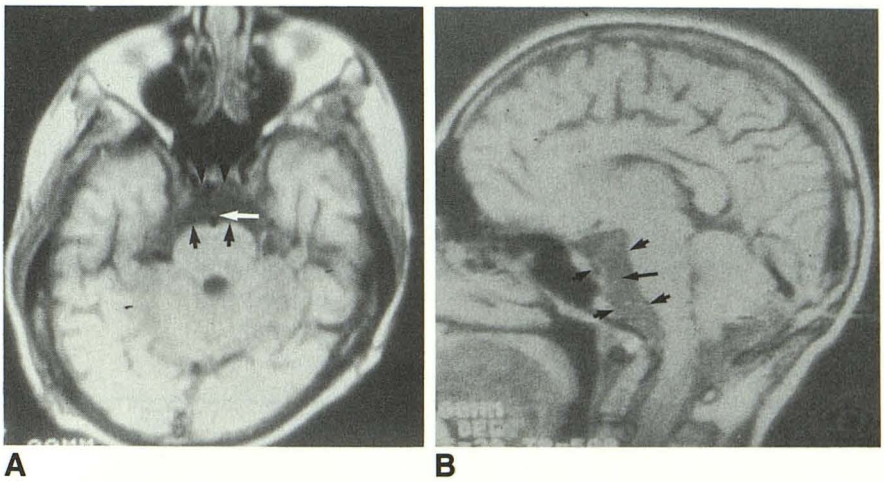

Fig. 8.—Suspected basal arachnoiditis.
A and *B*, Axial (*A*) and sagittal (*B*) MR images (500/28) show tissue thickening in basal meninges (*small arrows*) in case of hydrocephalus treated with ventriculoperitoneal shunt. *Large white arrow* in *A* points to basilar artery; *large black arrow* in *B* points to tissue thickness.

onstrated the presence of degenerative cysts with peripheral chronic inflammatory infiltration and gliosis.

In inactive NCC, the parenchymal calcifications were detected better by CT than by MR (23% vs 14%). Hydrocephalus was diagnosed equally well by each imaging method (25%), although the cause of the hydrocephalus was evident with MR in all cases. In 62.5% of the total cases in these series, two or more types of NCC were present.

There was a slight increase in proteins and leukocytes in the CSF with normal glucose values. The CSF changes were more prominent in spinal than in ventricular fluid. The ELISA in spinal CSF was positive in six of 10 patients (Table 1). The immunologic test against cysticercus in ventricular CSF was negative in all cases; however, in most of these, we were unable to obtain information about the methodology of the test.

Sixteen NCC cases were treated with ABZ. Three weeks after medical therapy, we observed complete disappearance of the lesions on MR follow-up in 13 patients (Table 2). Three cases had previous PZQ treatment with partial response. These findings suggest an ABZ effectiveness of 81%. Of nine PZQ-treated patients, seven were followed up with MR; four of these were normal, suggesting an effectiveness of 57%.

The cyst was surgically removed from the lateral or fourth ventricle in nine cases, from the brain parenchyma in five, and from the lumbar spine in one. Two patients with parenchymatous NCC had surgery because of mass effect; one case was in a supratentorial location and one in the cerebellum (Fig. 6).

Histologically, the live cysticercus had a multinucleated cellular layer (three-layered structure) with a scolex and no necrotic changes. These types of cysts were observed in most of the ventricular cysts. In three cases, degenerative changes were observed; the cysts appeared smaller in size and had thicker walls and hyalinized areas in some sections with remaining parts of the membranous structure. Gliosis and chronic inflammatory infiltration was observed in the periphery of these cysts (Fig. 9C). We have called this form degenerative cysticercus. Vasculitis or angiitis was histologically proved in one case of parenchymatous NCC (Fig. 10).

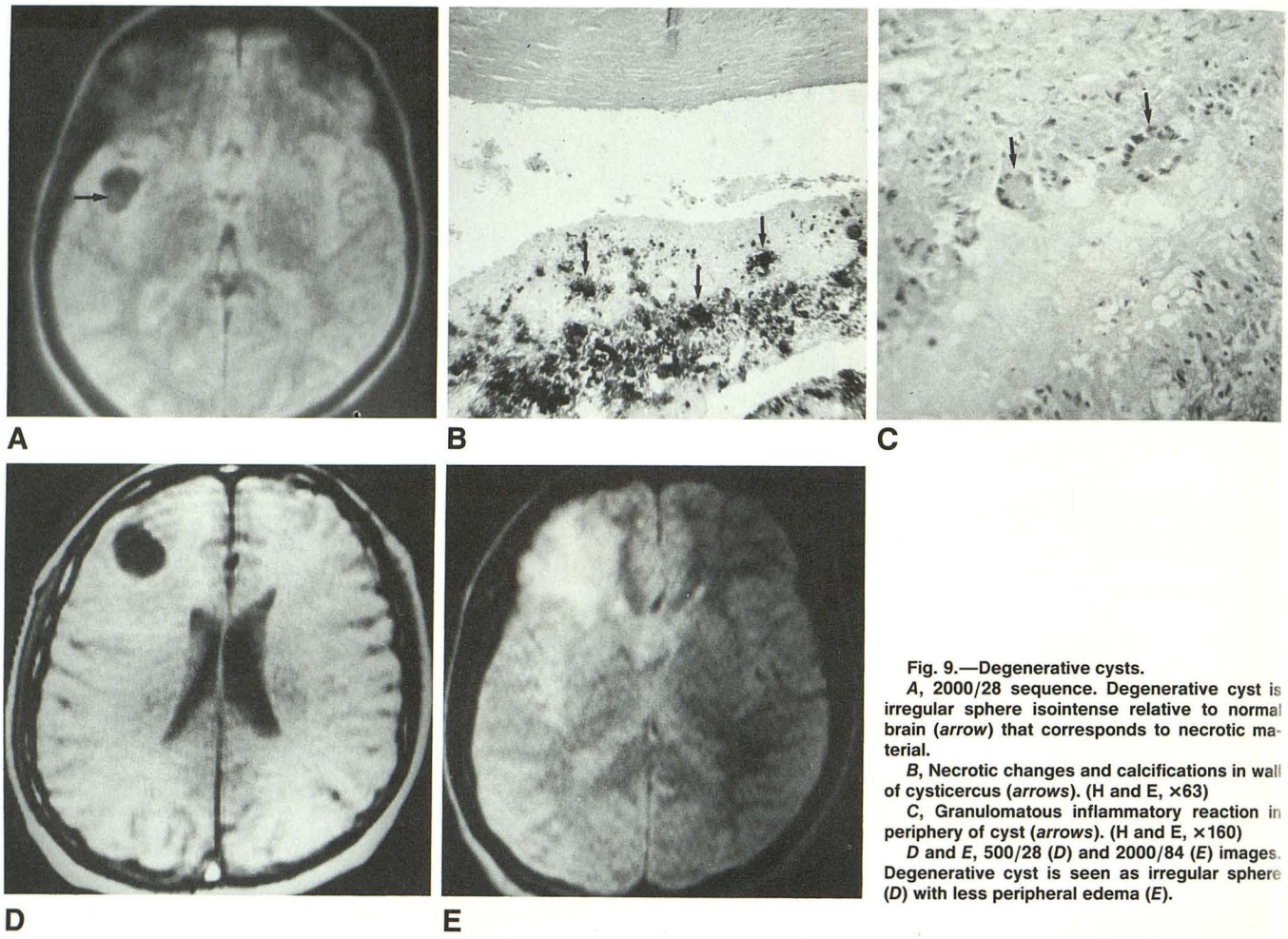

Fig. 9.—Degenerative cysts.

***A*, 2000/28 sequence. Degenerative cyst is irregular sphere isointense relative to normal brain (*arrow*) that corresponds to necrotic material.**

***B*, Necrotic changes and calcifications in wall of cysticercus (*arrows*). (H and E, ×63)**

***C*, Granulomatous inflammatory reaction in periphery of cyst (*arrows*). (H and E, ×160)**

***D* and *E*, 500/28 (*D*) and 2000/84 (*E*) images. Degenerative cyst is seen as irregular sphere (*D*) with less peripheral edema (*E*).**

TABLE 1: CSF Findings in Neurocysticercosis

Puncture Site/Case No.	Age	Gender	Glucose (mg/dl)	Protein (mg/dl)	Leukocytes (no./mm^3)	ELISA		Type of Neurocysticercosis
						CSF	Serum	
Lumbar								
1	16	F	53	43	13	+	−	Parenchymal cysts
2	47	M	60	85	8	+	+	Parenchymal, subarachnoid, and cisternal cysts
3	24	M	65	45	3	−	−	Parenchymal cysts
4	44	M	52	65	32	−	NA	Parenchymal, subarachnoid, and cisternal cysts
5	14	M	68	45	0	−	NA	Parenchymal cysts
6	19	F	20	200	800	+	+	Parenchymal cysts; meningeal involvement
7	47	M	52	40	0	−	−	Parenchymal cysts
8	46	M	40	78	4	+	NA	Subarachnoid cysts
9	43	F	74	15	2	+	−	Parenchymal cysts
10	37	F	80	45	6	+	−	Parenchymal and subarachnoid cysts
Ventricular								
11	34	M	50	32	0	−	NA	Ventricular
12	32	M	60	52	2	NA[a]	NA	Ventricular
13	32	M	36	45	6	NA[a]	NA	Ventricular; subarachnoid cysts
14	18	M	48	52	3	−	NA	Ventricular
15	23	F	NA	NA	NA	NA[a]	NA	Ventricular
16	42	F	NA	NA	NA	NA[a]	NA	Ventricular; parenchymal cysts
17	46	F	48	56	7	NA[a]	NA	Parenchymal and subarachnoid cysts; hydrocephalus
18	46	F	40	62	4	−	NA	Parenchymal cysts; hydrocephalus; aqueductal stenosis
19	19	F	38	42	0	−	+	Parenchymal cysts; aqueductal stenosis
20	26	M	29	46	0	NA[a]	−	Aqueductal stenosis

Note.—Normal values: glucose, >45 mg/dl; proteins, 20–45 mg/dl. Positive CSF titers are ≥1:8. ELISA = enzyme-linked immunosorbent assay; NA = not available.

[a] No information was provided about the methodology of determining antibodies against cysticercus.

TABLE 2: Treatment and Follow-up in Neurocysticercosis

Treatment/Location	No. of Cases	Gender	Mean Age	MR Follow-up Total/No. Normal
Surgical (n = 15)[a]				
Fourth ventricle	4	F	29	2/2
Lateral ventricle	5	F (1)	14	0/0
		M (4)	38	2/2
Parenchymal cysts	5	F (3)	34	2/0[b]
		M (2)	38	2/0[b]
Spinal cysts	1	M	65	1/0
Medical (n = 22)				
Praziquantel				
Parenchymal cysts	5	F (2)	18	2/2
		M (3)	36	2/1
Subarachnoid cysts	4	F (1)	19	1/0
		M (3)	53	2/1
Albendazole[c]				
Parenchymal cysts	9	F (4)	29	4/3
		M (5)	44	5/3
Mixed	4	F (1)	14	1/1
		M (3)	32	3/3
Subarachnoid cysts	3	F (2)	20	2/2
		M (1)	65	1/1

[a] Patients in whom a ventricular shunt catheter was placed are not included.
[b] No cysts were observed, but a high-intensity signal was detected in the operated area.
[c] Three patients were treated previously with praziquantel.

The racemose form appeared as a one-layer structure with an edematous wall and no scolex. Two examples of this form are illustrated in Figures 4A and 6. The ependymal and periependymal tissue samples showed inflammatory infiltration with periventricular edema. This inflammatory reaction was observed also in the arachnoid tissue of the sampled case.

Discussion

The human cysticercosis is usually produced by the encysted larva of the tapeworm *Taenia solium.* In autopsied cases, approximately two-thirds of the NCC cases are due to *Cysticercus cellulosae* and one-third are due to *Cysticercus racemose* [17].

The typical size of the *Cysticercus cellulosae* is 1 cm (ranging from 4–20 mm in diameter) and it has a characteristic rounded form. The fully developed parasite contains a round nodule measuring 2–3 mm that contains the scolex. The nodule is covered by a thin membrane (0.07–0.1 mm thick) within which there is a hyaline liquid. The cyst fluid has been described as transparent when the cysticercus is alive, turning turbid or "jellylike" with the death of the parasite [13, 18, 19].

The size of the *Cysticercus racemose* varies from 5 to 100 mm. Usually no scolex is found in this type of cyst. It is covered by a thin membrane showing irregularities in the inner layer. The peculiar size, shape, and absence of the scolex has led to speculation concerning its origin. Some authors believe this type of cyst is from a different type of *Taenia* or a degenerated form of *Taenia solium* larvae. Currently, the most accepted explanation is that the cysts lying in the subarachnoid space encounter less resistance around their walls than in the parenchyma, allowing the cysts to expand more freely and finally end up in a hydropic state [3, 18]. There is no particular explanation for the absence of the scolex, but it has been suggested that the scolex underwent degeneration, possibly in association with the hydropic state of the cysts.

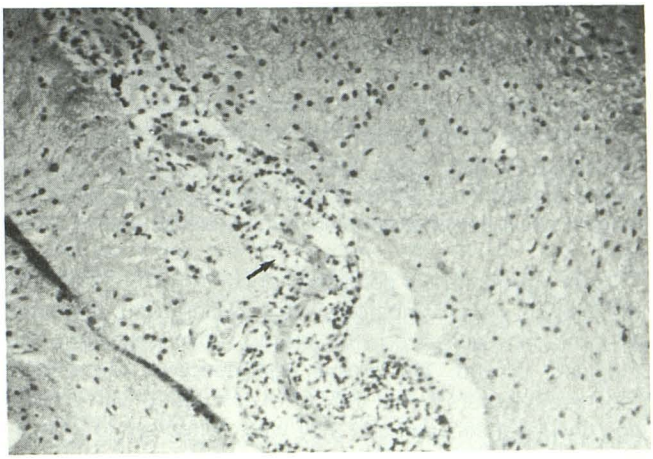

Fig. 10.—Vasculitic changes (*arrow*). (H and E, × 160)

The cysticercus has a marked tendency to lodge in the eye, muscle, and CNS [5]. This is attributed to the high content of glucose or glycogen and the rich vascular network in these organs [18].

Recently, the usefulness of MR in the evaluation of NCC has been reported [13, 14]. However, before MR was used, the diagnosis of NCC usually rested on CT and CSF findings. Immunologic studies of the CSF are frequently negative in intraventricular CSF [20] and probably in some patients with parenchymal NCC. With the advent of MR we have been able to diagnose NCC in locations previously undetected with other neuroimaging methods.

Of the 56 NCC cases described here, an active form was present in 85%. The most common presentation of active NCC was as parenchymal cysts, which is in agreement with previous reports [2, 5, 7, 9]. The MR configuration consisted of a vesicular structure with a fluid content having signal properties paralleling those of CSF. A high-intensity signal on T1-weighted images was observed inside the vesicle and corresponded to the scolex, an MR sign pathognomonic for NCC. When we compared MR with CT, we observed that MR was four times more sensitive in the detection of the cysts (85% vs 21%). An explanation for this is that MR could detect cysts in the brainstem, in a subependymal location, in the cerebellum (Fig. 6), in the subarachnoid space (Fig. 4), and inside the ventricles (Fig. 2). Bone and other artifacts on CT usually do not allow the identification of cysts in these areas.

A high-intensity signal was observed surrounding most of the parenchymal cysts on T2 sequences. This was considered to be brain edema. However, the hypertense signal also may be due to inflammatory infiltrate, endarteritis, and gliosis, findings observed microscopically in the periphery of the cysts [18, 21, 22]. An accelerated inflammatory response results from the death of the parasite [23], which can be observed after administration of the antiparasitic drugs (ABZ or PZQ)

[7] or in cases of spontaneous remission due to normal host immunologic reaction. Varying degrees of reaction around different cysts of the same host have been observed with CT, indicating that the lesions are in different stages of evolution. This was also observed by MR in some of our cases (Fig. 1). MR during or early after medical therapy showed a larger area of hyperintense signal around the cyst on T2-weighted images; we considered this finding compatible with an acute dying cyst.

Three patients in our series had uncontrolled seizures; the MR findings were compatible with degenerative cysticercus (irregular sphere, less edema, and no scolex) and were histologically proved. The clinical significance of the chronic degenerative cysts is that they were associated with persisting convulsive seizures and they were refractory to antiparasitic drugs (ABZ or PZQ).

Before MR, intraventricular NCC had been diagnosed through metrizamide CT ventriculography; however, this is an invasive method that could be associated with misdiagnosis in fourth ventricle cysts [20, 24]. In our series, CT ventriculography detected the ventricular cysts in all but one case, which corresponded to a patient with a fourth ventricle cyst. In one case the cyst in the lateral ventricle was not well defined, whereas it was observed on MR (Fig. 3). The detection of the scolex by MR was more precise in intraventricular NCC. Cyst mobility within the ventricles caused by changes in position from supine to prone was observed in two cases; this ventricular migration can be pathognomonic for intraventricular NCC, a finding described with other invasive radiologic methods [25, 26]. A high-intensity signal was observed in the ependymal layer in all cases of fourth ventricle cysts, and periependymal edema, which was proved through histologic analysis, was observed in three surgical cases. Hydrocephalus was present in all intraventricular forms and was treated with placement of a ventricular shunt catheter.

The subarachnoid form of NCC was observed in six cases; in two of these, the racemose type of cyst was present (Fig. 4A). The *Cysticercus racemose* usually displays a mild inflammatory reaction, despite the fact that the vesicles may be very large (Fig. 6). This type of cyst frequently is located in the basal cisterns or inside the sylvian fissure.

Intraocular cysts were present in two young women who also had parenchymal NCC. One of them was initially treated with PZQ at another hospital. This treatment resulted in the loss of the involved eye due to the exaggerated immunologic response resulting from the death of the parasite in this extraneural location.

Intraspinal NCC was detected in one patient with chronic back pain when MR showed multiple vesicular structures in the subarachnoid space. The surgical findings proved the parasitic origin. In our experience, the cysticercosis vasculitis was better detected by enhanced CT than by MR (Fig. 7).

ELISA for immunoglobulin M in spinal CSF was positive in 60% of the analyzed cases, most of then parenchymatous NCC (Table 1). In a recent study of 126 CSF samples from patients with active NCC [9], ELISA for immunoglobulin M was positive in 87% of the cases; however, the sensitivity of the test decreased to 75% when the cases of parenchymal cysts were considered as a separate group. The small number of CSF samples analyzed in our series could explain the differences in the sensitivity of the test. It has been described that ELISA for immunoglobulin M is more sensitive than ELISA for immunoglobulin G in the diagnosis of NCC [9]. In ventricular CSF, the ELISA was negative in all cases. The reasons for this failure could be the following: (1) the local production of globulins is higher in the subarachnoid space than within the ventricles, (2) the CSF sample obtained either during ventricular shunting or removal of the ventricular cyst was noninflammatory, and (3) the methodology of the test was unknown in several cases.

Surgical removal of the cysts is the treatment of choice in ventricular NCC. This is because the antiparasitic drugs cannot reach the ventricular CSF. In parenchymal NCC, surgical therapy can be an option in the presence of mass effect or persistence of uncontrolled focal or generalized seizures despite adequate drug therapy (antiepileptic or antiparasitic drugs).

In almost all previous reports [7, 10, 15], the effectiveness of the antiparasitic drugs (PZQ or ABZ) in the treatment of NCC was evaluated objectively through the results of CT in cases with parenchymal NCC, although this method may be inadequate for measuring drug efficacy.

Our results (Table 2) in 22 treated patients indicate a drug effectiveness of 57% with PZQ and 82% with ABZ (Fig. 4). These results are close to those reported by other authors [7, 10].

In conclusion, the cysticercus has an MR configuration of a vesicle with a high-intensity signal nodule (T1 and T2 sequences) inside the sphere that corresponds to the scolex. The chronic degenerative cyst appears as irregular vesicles with less peripheral edema and lacking a scolex (Fig. 9). Brain edema is observed around the cyst when MR is performed during medical therapy; we have called this finding an acute dying cyst. MR is a noninvasive and safe method for diagnosing ventricular NCC. MR is more effective than CT in the diagnosis of active NCC, whereas CT is superior to MR in the diagnosis of inactive NCC (characterized mostly by calcifications). In our experience, MR has proved to be the best primary imaging method in evaluating patients with suspected NCC.

REFERENCES

1. Sotelo J. Cysticercosis. *Arch Inst Nac Neurol Neurocirugia* **1987**;2:65–68
2. Rodriguez-Carbajal J, Palacios E, Azar-Kia B, Churchill R. Radiology of cysticercosis of the central nervous system including computed tomography. *Radiology* **1977**;125:127–131
3. Escobar A, Nieto D. Cysticercosis. In: Minkler J, ed. *Pathology of the nervous system;* vol. 3. New York: McGraw-Hill, **1972**;2507–2515
4. Gajdusek C. Introduction of *Taenia solium* into West New Guinea with a note on an epidemic of burns for cysticercus epilepsy in the Ekari people of the Wissel Lakes area. *Papua New Guinea Med J* **1978**;21:329–342
5. Sotelo J, Guerrero V, Rubio F. Neurocysticercosis: a new classification based on active and inactive forms. A study of 753 cases. *Arch Intern Med* **1985**;145:442–445
6. Schultz TS, Ascher GF. Cerebral cysticercosis occurrence in the immigrant population. *Neurosurgery* **1978**;3:164–168
7. Sotelo J, Escobedo F, Rodriguez-Carbajal J, Torres B, Rubio-Donnadieu F. Therapy of parenchymal brain cysticercosis with praziquantel. *N Engl J*

Med **1984**;310:1001–1007
8. Nieto D. Cysticercosis of the nervous system: diagnosis by means of the spinal fluid complement fixation test. *Neurology* **1956**;6:725–738
9. Rosas N, Sotelo J, Nieto D. ELISA in the diagnosis of neurocysticercosis. *Arch Neurol* **1986**;43:353–356
10. Escobedo F, Penagos P, Rodriguez J, Sotelo J. Albendazole therapy for neurocysticercosis. *Arch Intern Med* **1937**;147:738–741
11. Corona T, Pascoe D, Gonzalez-Barranco D, Abad P, Landa L, Estañol B. Anticysticercous antibodies in serum and cerebrospinal fluid in patients with cerebral cysticercosis. *J Neurol Neurosurg Psychiatry* **1986**;49:1044–1049
12. Barkovich AJ, Citrin CM, Klara P, Wippold FJ, Kattah J. Magnetic resonance imaging of cysticercosis. *West J Med* **1986**;145:687–690
13. Suss RA, Maravilla KR, Thompson J. MR imaging of intracranial cysticercosis: comparison with CT and anatomopathologic features. *AJNR* **1986**;7:235–242
14. Enzmann DR. *Imaging of infections and inflammations of the central nervous system: computed tomography, ultrasound, and nuclear magnetic resonance.* New York: Raven, **1984**:103–147
15. Vasconcelos D, Cruz-Segura H, Mateos-Gomez H, Zenteno Alanis G. Selective indications for the use of praziquantel in the treatment of brain cysticercosis. *J Neurol Neurosurg Psychiatry* **1987**;50:383–388
16. Gonzalez-Morantes J, Rangel-Guerra R, Campa H, Vogel H. Die Cysticercosis Cerebralis. *Comput Tomogr CT Sonographie* **1983**;3:87–92
17. Briseño EC, Biagi FF, Martínez B. Cisticercosis. Observaciones sobre 97 casos de autopsia. *Prensa Med Mex* **1958**;26:193–197
18. Escobar A. The pathology of neurocysticercosis. In: Palacios E, Rodriguez-Carbajal J, Taveras JM, eds. *Cysticercosis of the central nervous system.* Springfield, Il: Thomas, **1983**:27–54
19. Trelles JO, Trelles L. Cysticercosis of the nervous system. In: Vinken PJ, Bruyn GW, eds. *Handbook of clinical neurology,* vol. 35. Amsterdam: North-Holland, **1978**:291–320
20. Salazar A, Sotelo J, Martinez H, Escobedo F. Differential diagnosis between ventriculitis and fourth ventricle cyst in neurocysticercosis. *J Neurosurg* **1983**;59:660–663
21. Graw W, Garrido F, Cañedo L. Calcification of the cysticerci of *Taenia solium* in the human brain. In: Flisser A, Williams K, Laclette JP, Larralde C, Ridaura C, Beltran F, eds. *Cysticercosis: present state of knowledge and perspectives.* New York: Academic, **1982**:235–259
22. Ramirez-Bon E, Merchant MT, Gonzalez-Del Pliego M, Cañedo L. Ultrastructure of the bladder wall of the metacestode of *Taenia solium.* In: Flisser A, Williams K, Laclette JP, Larralde C, Ridaura C, Beltran F, eds. *Cysticercosis: present state of knowledge and perspectives.* New York: Academic, **1982**:261–280
23. Rabiels-Cervantes MT, Rivas-Hernandez A, Rodriguez-Ibarra J, Castillo-Medina S, Cancino F. Anatomopathological aspects of human brain cysticercosis. In: Flisser A, Williams K, Laclette JP, Larralde C, Ridaura C, Beltran F, eds. *Cysticercosis: present state of knowledge and perspectives.* New York: Academic, **1982**:179–200
24. Rangel-Guerra R, Herrera J, Elizondo G, Gonzalez-Morantes J. Neurocysticersosis. *Arch Neurol* **1988**;45:492
25. Zee CS, Segall HD, Apuzzo MLJ, Ahmadi J, Dobkin WR. Intraventricular cysticercal cysts: further neuroradiologic observations and neurosurgical implications. *AJNR* **1984**;5:727–730
26. Zee CS, Segall HD, Miller C, et al. Unusual neuroradiological features of intracranial cysticercosis. *Radiology* **1980**;137:397–407